The IRM Quarterly
Fall 2013, Vol. 23 No.3
ISSN: 2152-1972

Inside...

What do the Mumpsies do?

Dario Bilardello and Mike Jackson
IRM

A common challenge faced by most visitors to the IRM is familiarizing themselves with the measurement sequences that may be performed on the Magnetic Properties Measurement System instruments (MPMSs, built by Quantum Design Inc., San Diego), colloquially referred to in the lab as "The Mumpsies".

We have two mumpsies at the IRM (collective noun "mumble", e.g. *"a mumble of mumpsies"*, owing to the sanctuary-quiet liquefier that collects the helium boil off and converts it back to liquid), MPMS-XL ("*Big Red*") and MPMS-5S, ("*Old Blue*", often referred to as "*New Blue*", but that's another story).

The main use of the MPMS is to measure magnetization (both in-field and remanent) as a function of applied field and (low) temperature, with specific details programmed by the user. The temperature range is from 1.7 K to 400 K, applied fields can range from 0 to ± 5 T and variable frequency, in the range between mHz to kHz, though measurements at mHz frequencies take times that exceed average human tolerance. Measurements on older instruments were restricted to the heating steps, however more modern machines (like ours) can also measure during cooling. The measurement possibilities are limited only by one's imagination and the machine's specifications: in field and remanent magnetization curves, susceptibility curves and hysteresis loops being the fundamental building blocks.

Both instruments have many preset measurement sequences to choose from that have been designed by different users over the years, allowing investigating magnetic properties from room T or above (300 K *Old Blue* and 400 K *Big Red*) to low T (commonly 20, 10 or 5 K, with measurement time considerably increasing with decreasing T), with the capability of creating new *ad hoc* sequences, modifying and/or merging existing ones.

From a purely mechanical point of view, what such sequences actually do is not that straightforward and even less are the names that the different users have given to such sequences through the years ("*The big Lebowsky*"? "*The lesser Lebowsky*"??), hence the idea of writing a short note to shed some light on the mysterious ways of the mumpsies.

The interpretation of low temperature data was already extensively treated in a series of past Quarterly articles and will not be the focus here. Instead, this article will try to provide examples of the most characteristic features that we all ultimately hope to see when performing low temperature measurements.

"Flotsam and Jetsam" keep a close eye on all MPMS measurements.

Measurement Sequences

In the following, some of the most commonly used sequences will be described, which shall serve as a base for understanding the measurements and provide the tools for designing new sequences. For most f(T) experiments, the measurement interval is typically 5 or 10 K.

RTSIRM LTD

One of the most simple and rapid measurement sequences which may be performed involves imparting a saturation isothermal remanent magnetization (SIRM) at room (300 K) temperature (RTSIRM) and subsequently performing a low temperature demagnetization (LTD). The specimen is subject to a sustained DC field (typically 2.5 T) for a short amount of time (~1 minute) while at 300 K (lower graph in figure 1). Magnetic remanence measurements are performed as the specimen is cooled to the specified low temperature (most typically 20 K), and subsequently warmed back up to 300 K (upper graph in figure 1). The total duration of such a measurement is approximately 2.5 hours.

RTSIRM LTD experiments generate the RT remanence on cooling and RT remanence on heating curves (figure 2), which possess different shapes and spacing depending on magnetic mineralogy, oxidation and domain state (see Mineral Diagnostics paragraph below for details).

Advantages: rapid; characterizes phases capable of

cont'd. on pg. 11...

Visiting Fellows' Reports

An interdisciplinary approach to characterizing the hydrogeology of Blowing Spring Cave, northwestern Arkansas; exploring clastic cave sedimentation using paleomagnetism

Catherine Knierim
Department of Geosciences, University of Arkansas
kknierim@uark.edu

The preservation of chemical and clastic sediments in caves has provided proxy records for paleoclimate reconstructions using isotopic analyses (Denniston et al., 2007; Granger et al., 2001; Panno et al., 2004) and, more recently, magnetic susceptibility (Ellwood and Gose, 2006; Lascu and Feinberg, 2011). Cave sediments from sites in the midcontinent have been found to be millions of years old and extensively record climatic variations, specifically due to glacial-interglacial cycling (Granger et al., 2001; Panno et al., 2004). In the Ozark Physiographic Province (Ozarks), caves commonly contain clastic sediments ranging from chert and limestone cobbles to fine-grained material, such as insoluble clays. The source of Ozark cave sediments are generally Pleistocene loess or residuum from carbonate bedrock (Criss et al., 2009). To date, little has been published using cave sediments in the Ozarks (Denniston et al., 2007); however, broad questions can be answered using the novel approach of applying mineral magnetism to clastic cave sediments. For example, the age of Ozark caves is thought to be Pleistocene (Criss et al., 2009), but identifying sequences of normal versus reversed polarity in cave sediments at in the Ozarks could better constrain this hypothesis.

Blowing Spring Cave is located in the Ozarks of northwestern Arkansas and includes approximately 2,300 m of passage developed in the Mississippian Boone Formation. A cave stream flows through the cave and incised into clastic sedimentary deposits of mixed clay and chert gravel. Laminated clastic exposures can be found throughout the cave and deposits range in depth from <1 m to ~3 m thick. In the spring of 2013, three fully oriented U-channel sediment cores (1 to 1.5 m long) were collected from two sites in Blowing Springs Cave. The sediment deposits are fine-grained silts and clays and display millimeter and sub-millimeter laminations.

During my visit at the IRM, the natural remanent magnetization (NRM) of the sediment cores was measured using the 2G Enterprises superconducting rock magnetometer and several laboratory-induced magnetizations were imparted and demagnetized. The cores were also analyzed for magnetic susceptibility and light reflectance at the University of Minnesota's nearby LacCore facility. Additionally, approximately 5-cm interval sub-samples were collected from the cores for hysteresis measurements and low-temperature magnetometry using the Vibrating Sample Magnetometer (VSM, at room temperature) and the Quantum Designs Magnetic Property Measurement System (MPMS, at low temperatures). The analyses provided a "first look" at the clastic cave sediment to estimate variations in the concentration, composition, and grain size distributions of magnetic minerals with depth.

No paleomagnetic reversals were found in the Blowing Spring Cave sediment, but inclination and declination of magnetic minerals varied with depth, providing evidence that the magnetic minerals have recorded geomagnetic secular variation. Reconstructing the paleomagnetic record from primary remanent magnetism for the three cores is on-going, and once complete, the cores will be compared to paleomagnetic records from lake and ocean sediments to constrain the timing of sediment deposition in Blowing Spring Cave. A particular problem in many cave sediments is low organic carbon content, which prevents radiocarbon dating to better constrain the age of sediments and, therefore, the secular paleomagnetic record may provide a means to estimate the age of clastic sediment deposition. Based on MPMS measurements, the cores contain a mixture of soft-magnetic minerals, such as magnetite, and hard-magnetic minerals, such as goethite. The goethite remanence may present a problem as it formed via chemical precipitation in situ and likely holds a chemical remanent magnetization (CRM), as opposed to a detrital remanent magnetization (DRM). It is unclear if the goethite records the Earth's magnetic field at the time of sediment deposition in the cave, or at some subsequent time. As the data analyses are on-going, I am excited to continue the research to describe the magnetic mineral assemblage and reconstruct the paleomagnetic record for the cores. I would like to thank the IRM group for their warm welcome, incredible knowledge, and tasty coffee. I would especially like to thank Dr. Mike Jackson for his infinite patience and kindness in training me on the IRM instruments.

References

Criss, R. E., Osburn, R., and House, R.S., 2009, The Ozark Plateaus: Missouri, in eds. Palmer, A. N. and Palmer, M. V., Caves and Karst of the USA, National Speological Society, Inc., Huntsville, Alabama, p. 156-170.

Denniston, R.F., DuPree, M., Dorale, J.A., Asmerom, Y., Polyak, V.J., and Carpenter, S.J., 2007, Episodes of late Holocene aridity recorded by stalagmites from Devil's Icebox Cave, central Missouri, USA: Quaternary Research, v. 68, p. 45-52.

Ellwood, B. B., and Gose, W. A., 2006, Heinrich H1 and 8200 yr B.P. climate events recorded in Hall's Cave, Texas: Geology, v. 34, p. 753-756.

Granger, D. E., Fabel, D., Palmer, A. N., 2001, Pliocene-Pleis-

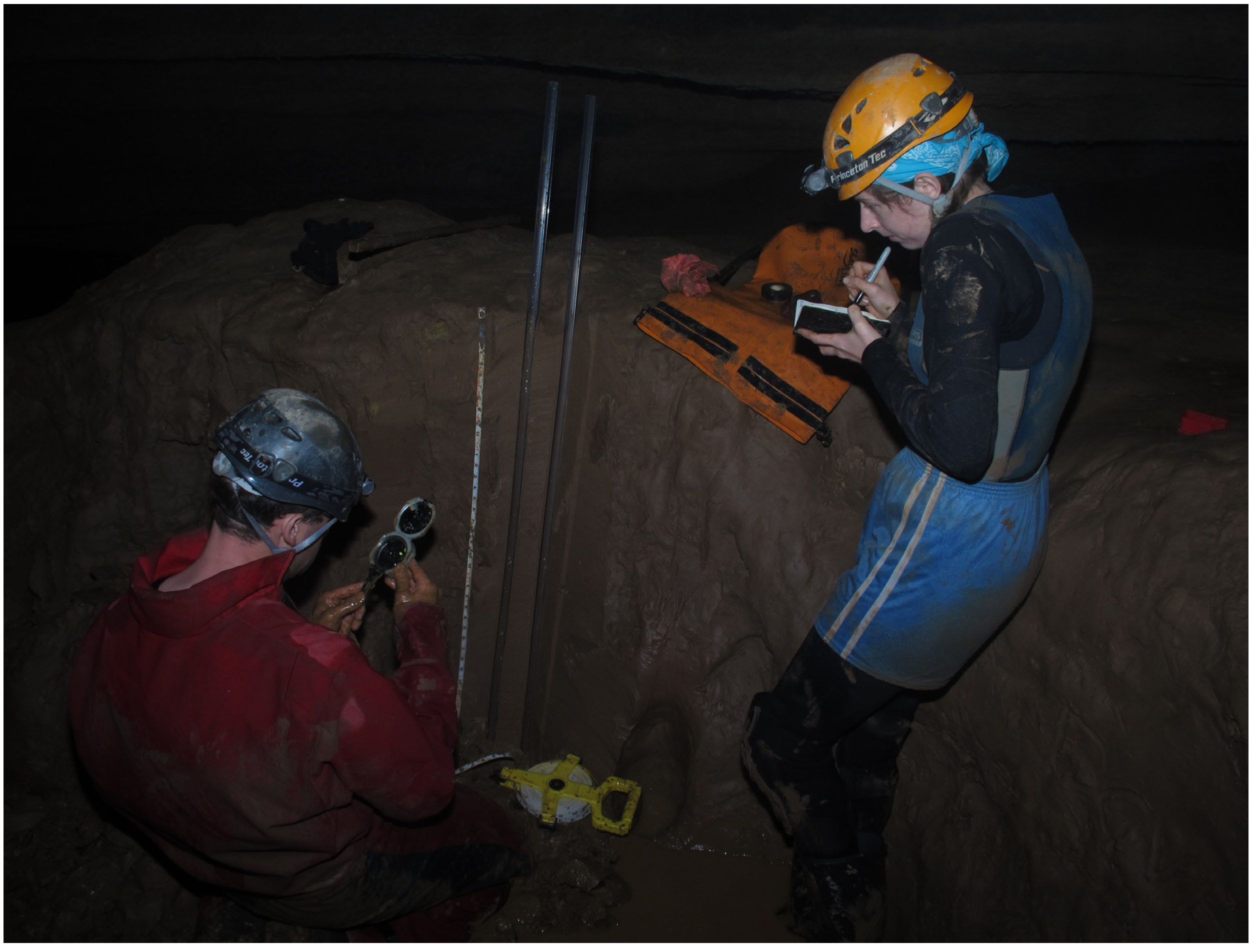

Fig 1. Catherine and IRM's Josh Feinberg doing the dirty work in Blowing Spring Cave, AR.

tocene incision of the Green River, Kentucky, determined from radioactive decay of cosmogenic 26Al and 10Be in Mammoth Cave sediments: GSA Bulletin, v. 113, p. 825-836.

Lascu, I. and Feinberg, J. M., 2011, Speleothem magnetism: Quaternary Science Reviews, v. 30, p. 3306-3320.

Panno, S. V., Curry, B. B., Wang, H., Hackley, K. C., Liu, C., Lundstrom, C., and Zhou, J., 2004, Climate change in southern Illinous, USA, based on the age and δ13C of organic matter in cave sediments: Quaternary Research, v. 61, p. 301-313.

The 2014 Santa Fe Conference on Rock Magnetism is approaching!

The 10th Santa Fe Conference on Rock magnetism will be help at St. John's College in Santa Fe New Mexico from June 26-30 2014. An optional field trip will be offered on Thursday June 26 and conference sessions will begin later that evening. On Sunday June 30th there will be an optional all day FORC worshop for those who wish to attend. Registration and travel information will be available soon on future issues of the IRM Quarterly, the IRM website and other media!

Current Articles

A list of current research articles dealing with various topics in the physics and chemistry of magnetism is a regular feature of the IRM Quarterly. Articles published in familiar geology and geophysics journals are included; special emphasis is given to current articles from physics, chemistry, and materials-science journals. Most are taken from ISI Web of Knowledge, after which they are subjected to Procrustean culling for this newsletter. An extensive reference list of articles (primarily about rock magnetism, the physics and chemistry of magnetism, and some paleomagnetism) is continually updated at the IRM. This list, with more than 10,000 references, is available free of charge. Your contributions both to the list and to the Current Articles section of the IRM Quarterly are always welcome.

Anisotropy and Magnetic Fabrics

Alimohammadian, H., Z. Hamidi, A. Aslani, A. Shahidi, F. Cifelli, and M. Mattei (2013), A tectonic origin of magnetic fabric in the Shemshak Group from Alborz Mts. (northern Iran), Journal of Asian Earth Sciences, 73, 419-428.

Cavalcante, G. C. G., M. Egydio-Silva, A. Vauchez, P. Camps, and E. Oliveira (2013), Strain distribution across a partially molten middle crust: Insights from the AMS mapping of the Carlos Chagas Anatexite, Aracuai belt (East Brazil), Journal of Structural Geology, 55, 79-100.

Haerinck, T., T. N. Debacker, and M. Sintubin (2013), Magnetic anisotropy of chloritoid, Journal of Geophysical Research-Solid Earth, 118(8), 3886-3898.

Moussaid, B., H. El Ouardi, A. Casas-Sainz, J. J. Villalain, T. Roman-Berdiel, B. Oliva-Urcia, R. Soto, and S. Torres-

Lopez (2013), Magnetic fabrics in the Jurassic-Cretaceous continental basins of the northern part of the Central High Atlas (Morocco): Geodynamic implications, Journal of African Earth Sciences, 87, 13-32.

Petronis, M. S., A. Delcamp, and B. V. de Vries (2013), Magma emplacement into the Lemptegy scoria cone (Chaine Des Puys, France) explored with structural, anisotropy of magnetic susceptibility, and Paleomagnetic data, Bulletin of Volcanology, 75(10).

Rosiere, C. A., O. L. Garcia, H. Siemes, and H. Schaeben (2013), Domainal fabrics of hematite in schistose, shear zone-hosted high-grade Fe ores: The product of the interplay between deformation and mineralization, Journal of Structural Geology, 55, 150-166.

Salazar, C. A., C. J. Archanjo, S. W. D. Rodrigues, M. Hollanda, and D. Y. Liu (2013), Age and magnetic fabric of the Trs Crregos granite batholith: evidence for Ediacaran transtension in the Ribeira Belt (SE Brazil), International Journal of Earth Sciences, 102(6), 1563-1581.

Archeomagnetism

Dill, H. G., A. Techmer, and J. Kus (2013), Evolution of an old mining district between 725 and 1630 AD at the boundary between Thuringen and Bayern, SE Germany, using mineralogical and chemical markers, radio-carbon dating, and coal petrography of slags, Archaeological and Anthropological Sciences, 5(3), 215-233.

Ech-Chakrouni, S., Hus, J., and Spassov, S. (2013), Constraints of archaeomagnetic dating and field intensity determinations in three ancient tile kilns in Belgium, Studia Geophysica et Geodaetica, 57, 4, 585-604.

Frahm, E., and J. M. Feinberg (2013), From flow to quarry: magnetic properties of obsidian and changing the scale of archaeological sourcing, Journal of Archaeological Science, 40(10), 3706-3721.

Gomes, H., P. Rosina, P. Holakooei, T. Solomon, and C. Vaccaro (2013), Identification of pigments used in rock art paintings in Gode Roriso-Ethiopia using Micro-Raman spectroscopy, Journal of Archaeological Science, 40(11), 4073-4082.

Morales, J., Goguitchaichvili, A., Ángeles Olay Barrientos, M., Carvallo, C., and Aguilar Reyes, B. (2013), Archeointensity investigation on pottery vestiges from Puertas de Rolón, Capacha culture: In search for affinity with other Mesoamerican pre-Hispanic cultures, Studia Geophysica et Geodaetica, 57, 4, 605-626.

Biomagnetism

Baumgartner, J., G. Morin, N. Menguy, T. P. Gonzalez, M. Widdrat, J. Cosmidis, and D. Faivre (2013), Magnetotactic bacteria form magnetite from a phosphate-rich ferric hydroxide via nanometric ferric (oxyhydr)oxide intermediates, Proceedings of the National Academy of Sciences of the United States of America, 110(37), 14883-14888.

Braunschweig, J., J. Bosch, and R. U. Meckenstock (2013), Iron oxide nanoparticles in geomicrobiology: from biogeochemistry to bioremediation, New Biotechnology, 30(6), 793-802.

Lefevre, C. T., et al. (2013), Comparative genomic analysis of magnetotactic bacteria from the Deltaproteobacteria provides new insights into magnetite and greigite magnetosome genes required for magnetotaxis, Environmental Microbiology, 15(10), 2712-2735.

Moreno, A. J., E. Gonzalez, M. Godoy, J. Pettinari, P. S. Antonel, G. Jorge, and V. Bekeris (2013), Spatial Resolution in Micrometric Periodic Assemblies of Magnetotactic Bacteria and Magnetic Nanoparticles, Ieee Transactions on Magnetics, 49(8), 4572-4575.

Strbak, O., P. Kopcansky, M. Timko, and I. Frollo (2013), Single Biogenic Magnetite Nanoparticle Physical Characteristics-A Biological Impact Study (For MagMeet 2012 Participants) (vol 49, pg 457, 2013), Ieee Transactions on Magnetics, 49(9), 5166-5168.

Chronostratigraphy/Magnetostratigraphy

Abrajevitch, A., R. S. Hori, and K. Kodama (2013), Rock magnetic record of the Triassic-Jurassic transition in pelagic bedded chert of the Inuyama section, Japan, Geology, 41(7), 803-806.

Best, M. G., E. H. Christiansen, A. L. Deino, S. Gromme, G. L. Hart, and D. G. Tingey (2013), The 36-18 Ma Indian Peak-Caliente ignimbrite field and calderas, southeastern Great Basin, USA: Multicyclic super-eruptions, Geosphere, 9(4), 864-950.

Bijl, P. K., A. Sluijs, and H. Brinkhuis (2013), A magneto- and chemostratigraphically calibrated dinoflagellate cyst zonation of the early Palaeogene South Pacific Ocean, Earth-Science Reviews, 124, 1-31.

Castro, J. M. B., M. Martinon-Torres, R. Blasco, J. Rosell, and E. Carbonell (2013), Continuity or discontinuity in the European Early Pleistocene human settlement: the Atapuerca evidence, Quaternary Science Reviews, 76, 53-65.

Djerrab, A., I. Hedley, P. Camps, S. Abdessadok, C. B. Ruiz, and D. B. Ortega (2013), Contribution of magnetic parameters to the identification of stratigraphic levels and pedogenesis (Angel Cave, Spain), Estudios Geologicos-Madrid, 69(1), 71-84.

Fu, C. F., Z. S. An, X. K. Qiang, J. Bloemendal, Y. G. Song, and H. Chang (2013), Magnetostratigraphic determination of the age of ancient Lake Qinghai, and record of the East Asian monsoon since 4.63 Ma, Geology, 41(8), 875-878.

Guerra-Merchan, A., F. Serrano, A. R. Bustos, M. Garces, J. M. Insua-Arevalo, and J. M. Garcia-Aguilar (2013), Approach to the Lower Pliocene marine-continental correlation from southern Spain. The micrommamal site of Alhaurin el Grande-1 (Malaga Basin, Betic Cordillera, Spain), Estudios Geologicos-Madrid, 69(1), 85-96.

Gulyuz, E., N. Kaymakci, M. J. M. Meijers, D. J. J. van Hinsbergen, C. Lefebvre, R. L. M. Vissers, B. W. H. Hendriks, and A. A. Peynircioglu (2013), Late Eocene evolution of the Cicekdagi Basin (central Turkey): Syn-sedimentary compression during microcontinent-continent collision in central Anatolia, Tectonophysics, 602, 286-299.

Lanci, L., E. Tohver, A. Wilson, and S. Flint (2013), Upper Permian magnetic stratigraphy of the lower Beaufort Group, Karoo Basin, Earth and Planetary Science Letters, 375, 123-134.

Perez-Gonzalez, A., J. L. Gallardo-Millan, D. U. del Val, J. Panera, and S. Rubio-Jara (2013), The Matuyama-Brunhes reversal at the river Jarama sequence of terraces between Velilla de San Antonio and Altos de la Mejorada, SE of Madrid (Spain), Estudios Geologicos-Madrid, 69(1), 35-46.

Wang, X. X., M. Zattin, J. J. Li, C. H. Song, S. Chen, C. Yang, S. D. Zhang, and J. W. Yang (2013), Cenozoic Tectonic Uplift History of Western Qinling: Evidence from Sedimentary and Fission-Track Data, Journal of Earth Science, 24(4), 491-505.

Computation and Development

Camacho, V., López-Rodríguez, D., Costanzo-Álvarez, V., Aldana, M., Hurtado, N., and Bayona, G. (2013), A neuro fuzzy approach to recognize rock magnetic and lithological patterns in a stratigraphic well from the Llanos Foreland Basin (Colombia), Studia Geophysica et Geodaetica, 57, 4, 669-691.

Francavilla, T. L., J. H. Claassen, and M. A. Willard (2013), A digital hysteresis loop experiment, American Journal of Physics, 81(10), 745-749.

Gailitis, A. (2013), Mathematical background of the Riga dynamo experiment, Geophysical and Astrophysical Fluid Dynamics, 107(4), 467-480.

Harres, A., R. Cichelero, L. G. Pereira, J. E. Schmidt, and J. Geshev (2013), Remanence plots technique extended to exchange bias systems, Journal of Applied Physics, 114(4).

Kohashi, T., and K. Motai (2013), Sample heating system for spin-polarized scanning electron microscopy, Microscopy, 62(4), 429-436.

Lee, S. J., S. Sato, T. Niizeki, H. Yanagihara, E. Kita, and C. Mitsumata (2013), Effect of calculation conditions on the numerical simulation of magnetic materials with random magnetic anisotropy, Journal of the Korean Physical Society, 63(3), 768-772.

Peralta, A., Costanzo-Alvarez, V., Carrillo, E., Durán, L.E, Aldana, M., and Rey, D. (2013), Numerical relationships between magnetic parameters measured in Quaternary sediments and global paleoclimatic proxies, Studia Geophysica et Geodaetica, 57, 4, 647-668.

Ramarotafika, R., A. Benabou, and S. Clenet (2013), Stochastic Jiles-Atherton model accounting for soft magnetic material variability, Compel-the International Journal for Computation and Mathematics in Electrical and Electronic Engineering, 32(5), 1679-1691.

Roldan, A., D. Santos-Carballal, and N. H. de Leeuw (2013), A comparative DFT study of the mechanical and electronic properties of greigite Fe3S4 and magnetite Fe3O4, Journal of Chemical Physics, 138(20).

Walton, S. K., K. Zeissler, W. R. Branford, and S. Felton (2013), MALTS: A Tool to Simulate Lorentz Transmission Electron Microscopy From Micromagnetic Simulations, Ieee Transactions on Magnetics, 49(8), 4795-4800.

Yun, T. S., Y. J. Jeong, K. Y. Kim, and K. B. Min (2013), Evaluation of rock anisotropy using 3D X-ray computed tomography, Engineering Geology, 163, 11-19.

Environmental Magnetism and Climate

Blowes, D. W., C. J. Ptacek, and J. L. Jambor (2013), Mineralogy of mine wastes and strategies for remediation, in Environmental Mineralogy Ii, edited by D. J. Vaughan and R. A. Wogelius, pp. 295-337.

Bondarenko, O. V., N. I. Blokhina, and T. Utescher (2013), Quantification of Calabrian climate in southern Primory'e, Far East of Russia - An integrative case study using multiple proxies, Palaeogeography Palaeoclimatology Palaeoecology, 386, 445-458.

Bucko, M. S., O. P. Mattila, A. Chrobak, G. Ziolkowski, B. Johanson, J. Cuda, J. Filip, R. Zboril, L. J. Pesonen, and M. Lepparanta (2013), Distribution of magnetic particulates in a roadside snowpack based on magnetic, microstructural and mineralogical analyses, Geophysical Journal International, 195(1), 159-175.

Chaparro, M. A. E., G. Suresh, V. Ramasamy, and A. M. Sinito (2013), Magnetic studies and elemental analysis of river sediments: a case study from the Ponnaiyar River (Southeastern India), Environmental Earth Sciences, 70(1), 201-213.

Chekli, L., S. Phuntsho, M. Roy, and H. K. Shon (2013), Characterisation of Fe-oxide nanoparticles coated with humic acid and Suwannee River natural organic matter, Science of the Total Environment, 461, 19-27.

Chiari, G. (2013), Mineralogy and cultural heritage conservation, in Environmental Mineralogy Ii, edited by D. J. Vaughan and R. A. Wogelius, pp. 405-439.

Da Silva, A. C., et al. (2013), Magnetic susceptibility as a high-resolution correlation tool and as a climatic proxy in Paleozoic rocks - Merits and pitfalls: Examples from the Devonian in Belgium, Marine and Petroleum Geology, 46, 173-189.

Fernandez-Caliani, J. C., J. D. de la Rosa, A. M. S. de la Campa, Y. Gonzalez-Castanedo, and S. Castillo (2013), Mineralogy of atmospheric dust impacting the Rio Tinto mining area (Spain) during episodes of high metal deposition, Mineralogical Magazine, 77(6), 2793-2810.

Frank, U., N. R. Nowaczyk, P. Minyuk, H. Vogel, P. Rosen, and M. Melles (2013), A 350 ka record of climate change from Lake El'gygytgyn, Far East Russian Arctic: refining the pattern of climate modes by means of cluster analysis, Climate of the Past, 9(4), 1559-1569.

Guo, X. L., X. M. Liu, P. Y. Li, B. Lu, H. Guo, Q. Chen, Z. Liu, and M. M. Ma (2013), The magnetic mechanism of paleosol S5 in the Baoji section of the southern Chinese Loess Plateau, Quaternary International, 306, 129-136.

Heermance, R. V., A. Pullen, P. Kapp, C. N. Garzione, S. Bogue, L. Ding, and P. P. Song (2013), Climatic and tectonic controls on sedimentation and erosion during the Pliocene-Quaternary in the Qaidam Basin (China), Geological Society of America Bulletin, 125(5-6), 833-856.

Hiemstra, T., S. Mia, P. B. Duhaut, and B. Molleman (2013), Natural and Pyrogenic Humic Acids at Goethite and Natural Oxide Surfaces Interacting with Phosphate, Environmental Science & Technology, 47(16), 9182-9189.

Igwe, C. A., M. Zarei, and K. Stahr (2013), Stability of aggregates of some weathered soils in south-eastern Nigeria in relation to their geochemical properties, Journal of Earth System Science, 122(5), 1283-1294.

Jimenez-Moreno, G., F. Burjachs, I. Exposita, O. Oms, A. Carrancho, J. J. Villalain, J. Agusti, G. Campeny, B. G. de Soler, and J. van der Made (2013), Late Pliocene vegetation and orbital-scale climate changes from the western Mediterranean area, Global and Planetary Change, 108, 15-28.

Maul, L. C., et al. (2013), Age and palaeoenvironment of the enigmatic Arternian Interglacial - Evidence from the Muschelton at Voigtstedt/Hackelsberg (Thuringia, Central Germany), Palaeogeography Palaeoclimatology Palaeoecology, 386, 68-85.

Muttoni, G., E. Dallanave, and J. E. T. Channell (2013), The drift history of Adria and Africa from 280 Ma to Present, Jurassic true polar wander, and zonal climate control on Tethyan sedimentary facies, Palaeogeography Palaeoclimatology Palaeoecology, 386, 415-435.

Petrovský, E., Zbořil, R,. Grygar, T.M., Kotlík, B., Novák, J., Kapička, A., and Grison, H. (2013), Magnetic particles in atmospheric particulate matter collected at sites with different level of air pollution, Studia Geophysica et Geodaetica, 57, 4, 755-770.

Reyes, B.A., Mejía,V., Goguitchaichvili, A., Escobar, J., Bayona, G., Bautista, F., Morales, J.C., and Ihl, T.J., (2013). Reconnaissance environmental magnetic study of urban soils, dust and leaves from Bogotá, Colombia, Studia Geophysica et Geodaetica, 57, 4, 741-754.

Roberts, D. L., L. Sciscio, A. I. R. Herries, L. Scott, M. K. Bamford, C. Musekiwa, and H. Tsikos (2013), Miocene fluvial systems and palynofloras at the southwestern tip of Africa: Implications for regional and global fluctuations in climate and ecosystems, Earth-Science Reviews, 124, 184-201.

Sandler, A. (2013), Clay distribution over the landscape of Israel: From the hyper-arid to the Mediterranean climate regimes, Catena, 110, 119-132.

Sangode, S. J., S. Rawat, D. C. Meshram, N. R. Phadtare, and N. Suresh (2013), Integrated Mineral Magnetic and Lithologic Studies to Delineate Dynamic Modes of Depositional Conditions in the Leh Valley Basin, Ladakh Himalaya, India,

Journal of the Geological Society of India, 82(2), 107-120.

Sun, G. Y., Y. P. Chen, X. Y. Bi, W. Yang, X. S. Chen, Z. Bin, and Y. J. Cui (2013), Geochemical assessment of agricultural soil: A case study in Songnen-Plain (Northeastern China), Catena, 111, 56-63.

Tema, E, Kondopoulou, D., and Pavlides, S. (2013), Palaeotemperature estimation of the pyroclastic deposit covering the pre-Minoan palaeosol at Megalochori Quarry, Santorini (Greece): Evidence from magnetic measurements, Studia Geophysica et Geodaetica, 57, 4, 627-646.

Turner, D. G., B. C. Ward, J. D. Bond, B. J. L. Jensen, D. G. Froese, A. M. Telka, G. D. Zazula, and N. H. Bigelow (2013), Middle to Late Pleistocene ice extents, tephrochronology and paleoenvironments of the White River area, southwest Yukon, Quaternary Science Reviews, 75, 59-77.

Wang, R. J., W. S. Xiao, C. Marz, and Q. Y. Li (2013), Late Quaternary paleoenvironmental changes revealed by multi-proxy records from the Chukchi Abyssal Plain, western Arctic Ocean, Global and Planetary Change, 108, 100-118.

Wang, B., D. S. Xia, Y. Yu, J. Jia, and S. J. Xu (2013), Magnetic properties of river sediments and their relationship with heavy metals and organic matter in the urban area in Lanzhou, China, Environmental Earth Sciences, 70(2), 605-614.

Xie, S. C., et al. (2013), Concordant monsoon-driven postglacial hydrological changes in peat and stalagmite records and their impacts on prehistoric cultures in central China, Geology, 41(8), 827-830.

Zhu, Z. M., G. Y. Sun, X. Y. Bi, Z. G. Li, and G. H. Yu (2013), Identification of trace metal pollution in urban dust from kindergartens using magnetic, geochemical and lead isotopic analyses, Atmospheric Environment, 77, 9-15.

Extraterrestrial and planetary magnetism

Bish, D. L., et al. (2013), X-ray Diffraction Results from Mars Science Laboratory: Mineralogy of Rocknest at Gale Crater, Science, 341(6153).

Demory, F., P. Rochette, J. Gattacceca, T. Gabriel, and N. S. Bezaeva (2013), Remanent magnetization and coercivity of rocks under hydrostatic pressure up to 1.4GPa, Geophysical Research Letters, 40(15), 3858-3862.

Fares, R., C. Moutou, J. F. Donati, C. Catala, E. L. Shkolnik, M. M. Jardine, A. C. Cameron, and M. Deleuil (2013), A small survey of the magnetic fields of planet-host stars, Monthly Notices of the Royal Astronomical Society, 435(2), 1451-1462.

Lillis, R. J., S. T. Stewart, and M. Manga (2013), Demagnetization by basin-forming impacts on early Mars: Contributions from shock, heat, and excavation, Journal of Geophysical Research-Planets, 118(5), 1045-1062.

Maharaj, D., T. Elbra, and L. J. Pesonen (2013), Physical properties of the drill core from the El'gygytgyn impact structure, NE Russia, Meteoritics & Planetary Science, 48(7), 1130-1142.

Marrocchi, Y., and G. Libourel (2013), Sulfur and sulfides in chondrules, Geochimica Et Cosmochimica Acta, 119, 117-136.

Rietmeijer, F. J. M. (2013), An igneous fragment from cluster IDP L2011#21: An analog for the source of pyrrhotite and taenite in comet 81P/Wild 2 captured in Stardust aerogel, Meteoritics & Planetary Science, 48(8), 1427-1439.

Sabbah, I. (2013), Solar magnetic polarity dependency of the cosmic ray diurnal variation, Journal of Geophysical Research-Space Physics, 118(8), 4739-4747.

Schwenzer, S. P., and D. A. Kring (2013), Alteration minerals in impact-generated hydrothermal systems - Exploring host rock variability, Icarus, 226(1), 487-496.

Tao, R. B., Y. W. Fei, and L. F. Zhang (2013), Experimental determination of siderite stability at high pressure, American Mineralogist, 98(8-9), 1565-1572.

Zhang, N., E. M. Parmentier, and Y. Liang (2013), A 3-D numerical study of the thermal evolution of the Moon after cumulate mantle overturn: The importance of rheology and core solidification, Journal of Geophysical Research-Planets, 118(9), 1789-1804.

Magnetic Field Records and Paleointensity Methods

Aubert, J., C. C. Finlay, and A. Fournier (2013), Bottom-up control of geomagnetic secular variation by the Earth's inner core, Nature, 502(7470), 219.

Barbas, B. F. D., A. G. Elias, I. Cnossen, and M. Z. de Artigas (2013), Long-term changes in solar quiet (Sq) geomagnetic variations related to Earth's magnetic field secular variation, Journal of Geophysical Research-Space Physics, 118(6), 3712-3718.

Brown, W. I., J. E. Mound, and P. W. Livermore (2013), Jerks abound: An analysis of geomagnetic observatory data from 1957 to 2008, Physics of the Earth and Planetary Interiors, 223, 62-76.

Buffett, B. A., L. Ziegler, and C. G. Constable (2013), A stochastic model for palaeomagnetic field variations, Geophysical Journal International, 195(1), 86-97.

Calvo-Rathert, M., M. F. Bogalo, A. Gogichaishvili, J. Sologashvili, and G. Vashakidze (2013), New paleomagnetic and paleointensity data from Pliocene lava flows from the Lesser Caucasus, Journal of Asian Earth Sciences, 73, 347-361.

Channell, J. E. T., D. A. Hodell, V. Margari, L. C. Skinner, P. C. Tzedakis, and M. S. Kesler (2013), Biogenic magnetite, detrital hematite, and relative paleointensity in Quaternary sediments from the Southwest Iberian Margin, Earth and Planetary Science Letters, 376, 99-109.

Kulakov, E.V. and Smirnov, A.V. (2013), Absolute geomagnetic paleointensity as recorded by ~1.09 Ga Lake Shore Traps (Keweenaw Peninsula, Michigan), Studia Geophysica et Geodaetica, 57, 4, 565-584.

Korte, M., and R. Muscheler (2012), Centennial to millennial geomagnetic field variations, Journal of Space Weather and Space Climate, 2, doi: 10.1051/swsc/2012006.

Lappe, S., R. J. Harrison, J. M. Feinberg, and A. Muxworthy (2013), Comparison and calibration of nonheating paleointensity methods: A case study using dusty olivine, Geochemistry Geophysics Geosystems, 14(7), 2143-2158.

Mochizuki, N., T. Maruuchi, Y. Yamamoto, and H. Shibuya (2013), Multi-level consistency tests in paleointensity determinations from the welded tuffs of the Aso pyroclastic-flow deposits, Physics of the Earth and Planetary Interiors, 223, 40-54.

Muxworthy, A. R., M. E. Evans, S. J. Scourfield, and J. G. King (2013), Paleointensity results from the late-Archaean Modipe Gabbro of Botswana, Geochemistry Geophysics Geosystems, 14(7), 2198-2205.

Ohneiser, C., G. Acton, J. E. T. Channell, G. S. Wilson, Y. Yamamoto, and T. Yamazaki (2013), A middle Miocene relative paleointensity record from the Equatorial Pacific, Earth and Planetary Science Letters, 374, 227-238.

Poletti, W., G. A. Hartmann, M. J. Hill, A. J. Biggin, and R. I. F. Trindade (2013), The cooling-rate effect on microwave archeointensity estimates, Geophysical Research Letters, 40(15), 3847-3852.

Pope, E. C., D. K. Bird, and S. Arnorsson (2013), Evolution of low-O-18 Icelandic crust, Earth and Planetary Science Letters, 374, 47-59.

Roberts, P. H., and E. M. King (2013), On the genesis of the

Earth's magnetism, Reports on Progress in Physics, 76(9).

Takeda, M. (2013), Contribution of wind, conductivity, and geomagnetic main field to the variation in the geomagnetic Sq field, Journal of Geophysical Research-Space Physics, 118(7), 4516-4522.

Mineralogy and Petrology

Almeev, R. R., F. Holtz, A. A. Ariskin, and J. I. Kimura (2013), Storage conditions of Bezymianny Volcano parental magmas: results of phase equilibria experiments at 100 and 700 MPa, Contributions to Mineralogy and Petrology, 166(5), 1389-1414.

Blatter, D. L., T. W. Sisson, and W. Ben Hankins (2013), Crystallization of oxidized, moderately hydrous arc basalt at mid- to lower-crustal pressures: implications for andesite genesis, Contributions to Mineralogy and Petrology, 166(3), 861-886.

Bowles, J. F. W., H. M. Prichard, S. Suarez, and P. C. Fisher (2013), The first report of platinum-group minerals in magnetite-bearing gabbro, Freetown Layered Complex, Sierra Leone: occurrences and genesis, Canadian Mineralogist, 51(3), 455-473.

Burgess, K. D., and R. F. Cooper (2013), Extended planar defects and the rapid incorporation of Ti4+ into olivine, Contributions to Mineralogy and Petrology, 166(4), 1223-1233.

Cabral, A. R., and C. A. Rosiere (2013), The chemical composition of specular hematite from Tilkerode, Harz, Germany: implications for the genesis of hydrothermal hematite and comparison with the Quadrilatero Ferrifero of Minas Gerais, Brazil, Mineralium Deposita, 48(7), 907-924.

Cabral, A. R., N. Koglin, H. Strauss, H. Bratz, and R. Kwitko-Ribeiro (2013), Regional sulfate-hematite-sulfide zoning in the auriferous Mariana anticline, Quadrilatero Ferrifero of Minas Gerais, Brazil, Mineralium Deposita, 48(7), 805-816.

Tomiya, A., I. Miyagi, G. Saito, and N. Geshi (2013), Short time scales of magma-mixing processes prior to the 2011 eruption of Shinmoedake volcano, Kirishima volcanic group, Japan, Bulletin of Volcanology, 75(10).

Mineral Physics and Chemistry

Arantes, F. R., and D. R. Cornejo (2013), Monte Carlo study of the magnetic properties of frozen and non-interacting nanoparticles, Journal of Nanoparticle Research, 15(9).

Bolanz, R. M., M. Wierzbicka-Wieczorek, M. Caplovicova, P. Uhlik, J. Gottlicher, R. Steininger, and J. Majzlan (2013), Structural Incorporation of As5+ into Hematite, Environmental Science & Technology, 47(16), 9140-9147.

Bryant, B., A. Spinelli, J. J. T. Wagenaar, M. Gerrits, and A. F. Otte (2013), Local Control of Single Atom Magnetocrystalline Anisotropy, Physical Review Letters, 111(12).

Chakrabarty, S., and K. Chatterjee (2013), Oriented growth of alpha-Fe2O3 nanocrystals with different morphology and their optical behavior, Journal of Crystal Growth, 381, 107-113.

De Ranieri, E., et al. (2013), Piezoelectric control of the mobility of a domain wall driven by adiabatic and non-adiabatic torques, Nature Materials, 12(9), 808-814.

Gomaa, M. M. (2013), Forward and inverse modelling of the electrical properties of magnetite intruded by magma, Egypt, Geophysical Journal International, 194(3), 1527-1540.

Hillion, A., A. Tamion, F. Tournus, O. Gaier, E. Bonet, C. Albin, and V. Dupuis (2013), Advanced magnetic anisotropy determination through isothermal remanent magnetization of nanoparticles, Physical Review B, 88(9).

Krutyanskiy, V. L., I. A. Kolmychek, B. A. Gribkov, E. A. Karashtin, E. V. Skorohodov, and T. V. Murzina (2013), Second harmonic generation in magnetic nanoparticles with vortex magnetic state, Physical Review B, 88(9).

Lee, J., and S. Han (2013), Thermodynamics of native point defects in alpha-Fe2O3: an ab initio study, Physical Chemistry Chemical Physics, 15(43), 18906-18914.

Liu, H. B., T. H. Chen, X. H. Zou, C. S. Qing, and R. L. Frost (2013), Thermal treatment of natural goethite: Thermal transformation and physical properties, Thermochimica Acta, 568, 115-121.

Lutzenkirchen, J., T. Preocanin, F. Stipic, F. Heberling, J. Rosenqvist, and N. Kallay (2013), Surface potential at the hematite (001) crystal plane in aqueous environments and the effects of prolonged aging in water, Geochimica Et Cosmochimica Acta, 120, 479-486.

Machek, M., Roxerová, Z., Janoušek, V., Staněk, M., Petrovský, E., and René, M. (2013), Petrophysical and geochemical constraints on alteration processes in granites, Studia Geophysica et Geodaetica, 57, 4, 710-740.

Martinez-Sanchez, E. J. Lede, R. Martinez-Garcia, and L. M. Socolovsky (2013), Magnetic Properties of gamma - Fe2O3 Nanoparticles at the Verge of Nucleation Process, Ieee Transactions on Magnetics, 49(8), 4555-4558.

Ren, Z. S., X. J. Hu, X. X. Xue, and K. C. Chou (2013), Solid state reaction studies in Fe3O4-TiO2 system by diffusion couple method, Journal of Alloys and Compounds, 580, 182-186.

Sabsabi, Z., F. Vernay, O. Iglesias, and H. Kachkachi (2013), Interplay between surface anisotropy and dipolar interactions in an assembly of nanomagnets, Physical Review B, 88(10).

Sbiaa, R. (2013), Magnetization switching by spin-torque effect in off-aligned structure with perpendicular anisotropy, Journal of Physics D-Applied Physics, 46(39).

Rock and Mineral Magnetism

Anchuela, Ó.P., Pocovì, A.J., Imaz, A.G., and Casas-Sainz, A. (2013), Factors influencing magnetic susceptibility in the southern Pyrenees, Studia Geophysica et Geodaetica, 57, 4, 692-709.

Bisig, A., et al. (2013), Correlation between spin structure oscillations and domain wall velocities, Nature Communications, 4.

Cuda, J., T. Kohout, J. Filip, J. Tucek, A. Kosterov, J. Haloda, R. Skala, E. Santala, I. Medrik, and R. Zboril (2013), Low-temperature magnetism of alabandite: Crucial role of surface oxidation, American Mineralogist, 98(8-9), 1550-1556.

Franco, D. G., R. E. Carbonio, and G. Nieva (2013), Change in the Magnetic Domain Alignment Process at the Onset of a Frustrated Magnetic State in Ferrimagnetic La2Ni(Ni1/3Sb2/3)O-6 Double Perovskite, Ieee Transactions on Magnetics, 49(8), 4656-4659.

Kind, J., I. Garcia-Rubio, M. Charilaou, N. R. Nowaczyk, J. F. Loffler, and A. U. Gehring (2013), Domain-wall dynamics in 4C pyrrhotite at low temperature, Geophysical Journal International, 195(1), 192-199.

Kronseder, M., M. Buchner, H. G. Bauer, and C. H. Back (2013), Dipolar-energy-activated magnetic domain pattern transformation driven by thermal fluctuations, Nature Communications, 4.

Ma, M. M., X. M. Liu, B. J. Pillans, S. Y. Hu, B. Lu, and H. F. Liu (2013), Magnetic properties of Dashing Rocks loess at Timaru, South Island, New Zealand, Geophysical Journal International, 195(1), 75-85.

Maldonado, K. L. L., P. de la Presa, E. F. Tavizon, J. R. F. Mancilla, J. A. M. Aquino, A. H. Grande, and J. T. E. Galindo (2013), Magnetic susceptibility studies of the spin-glass and Verwey transitions in magnetite nanoparticles, Journal of

Applied Physics, 113(17).

McCollom, T. M., B. M. Hynek, K. Rogers, B. Moskowitz, and T. S. Berquo (2013), Chemical and mineralogical trends during acid-sulfate alteration of pyroclastic basalt at Cerro Negro volcano and implications for early Mars, Journal of Geophysical Research-Planets, 118(9), 1719-1751.

Mino, M., and Y. Yamamoto (2013), Chaotic motion of a magnetic domain structure under an alternating field, Journal of the Korean Physical Society, 63(3), 605-607.

Petrenko, O. A., M. R. Lees, and G. Balakrishnan (2013), Low-temperature magnetisation process in the cubic pyrochlore quantum antiferromagnet, Er2Ti2O7, European Physical Journal B, 86(10).

Salminen, J., L. J. Pesonen, K. Lahti, and K. Kannus (2013), Lightning-induced remanent magnetization-the Vredefort impact structure, South Africa, Geophysical Journal International, 195(1), 117-129.

Yang, T., J. Y. Chen, X. S. Yang, H. Q. Wang, and H. Q. Jin (2013), Differences in magnetic properties of fragments and matrix of breccias from the rupture of the 2008 Wenchuan earthquake, China: Relationship to faulting, Tectonophysics, 601, 112-124.

Paleomagnetism and Tectonics

Agirrezabala, L. M., and J. Dinares-Turell (2013), Albian syn-depositional block rotation and its geological consequences, Basque-Cantabrian Basin (western Pyrenees), Geological Magazine, 150(6), 986-1001.

Arriagada, C., R. Ferrando, L. Cordova, D. Morata, and P. Roperch (2013), The Maipo Orocline: A first scale structural feature in the Miocene to Recent geodynamic evolution in the central Chilean Andes, Andean Geology, 40(3), 419-437.

Bilardello, D. (2013), Understanding DRM acquisition of plates and spheres: a first comparative experimental approach, Geophysical Journal International, 195(1), 148-158.

Chi, C. T., and J. W. Geissman (2013), A review of the paleomagnetic data from Cretaceous to lower Tertiary rocks from Vietnam, Indochina and South China, and their implications for Cenozoic tectonism in Vietnam and adjacent areas, Journal of Geodynamics, 69, 54-64.

Cinku, M. C., Z. M. Hisarli, N. Orbay, T. Ustaomer, A. M. Hirt, S. Kravchenko, O. Rusakov, and N. Sayin (2013), Evidence of Early Cretaceous remagnetization in the Crimean Peninsula: a palaeomagnetic study from Mesozoic rocks in the Crimean and Western Pontides, conjugate margins of the Western Black Sea, Geophysical Journal International, 195(2), 821-843.

Darin, M. H., and R. J. Dorsey (2013), Reconciling disparate estimates of total offset on the southern San Andreas fault, Geology, 41(9), 975-978.

Edel, J. B., K. Schulmann, E. Skrzypek, and A. Cocherie (2013), Tectonic evolution of the European Variscan belt constrained by palaeomagnetic, structural and anisotropy of magnetic susceptibility data from the Northern Vosges magmatic arc (eastern France), Journal of the Geological Society, 170(5), 785-804.

Emmerton, S., A. R. Muxworthy, and M. A. Sephton (2013), A magnetic solution to the Mupe Bay mystery, Marine and Petroleum Geology, 46, 165-172.

Gurer, O. F., E. Sangu, M. Ozburan, A. Gurbuz, and N. Sarica-Filoreau (2013), Complex basin evolution in the Gokova Gulf region: implications on the Late Cenozoic tectonics of southwest Turkey, International Journal of Earth Sciences, 102(8), 2199-2221.

Hoshi, H., N. Kamiya, and Y. Kawakami (2013), Instantaneous paleomagnetic record from the Miocene Kozagawa Dike of the Kumano Acidic Rocks, Kii Peninsula, Southwest Japan: cautionary note on tectonic interpretation, Island Arc, 22(3), 395-409.

Huang, W. T., G. Dupont-Nivet, P. C. Lippert, D. J. J. van Hinsbergen, and E. Hallot (2013), Inclination shallowing in Eocene Linzizong sedimentary rocks from Southern Tibet: correction, possible causes and implications for reconstructing the India-Asia collision, Geophysical Journal International, 194(3), 1390-1411.

Iosifidi, A. G., and A. N. Khramov (2013), Paleomagnetism of Devonian and Carboniferous sedimentary rocks of Spitsbergen: to the Paleozoic history of the Barents-Kara basin framing, Izvestiya-Physics of the Solid Earth, 49(5), 725-742.

Johnston, S. T., A. B. Weil, and G. Gutierrez-Alonso (2013), Oroclines: Thick and thin, Geological Society of America Bulletin, 125(5-6), 643-663.

Kirscher, U., A. Zwing, D. V. Alexeiev, H. P. Echtler, and V. Bachtadse (2013), Paleomagnetism of Paleozoic sedimentary rocks from the Karatau Range, Southern Kazakhstan: Multiple remagnetization events correlate with phases of deformation, Journal of Geophysical Research-Solid Earth, 118(8), 3871-3885.

Kristjansson, L. (2013), Analyses of primary remanence vector data from a large collection of lava flows: towards improved methodology in paleo-geomagnetism, Studia Geophysica et Geodaetica, 57, 4, 543-564.

Lee, B., W. H. Ryang, and S. J. Doh (2013), Paleomagnetism on the Quaternary marine sediment at the DH-1 long-core site in the Korean continental margin of the East Sea, Geosciences Journal, 17(3), 279-287.

Li, Z. X., D. A. D. Evans, and G. P. Halverson (2013), Neoproterozoic glaciations in a revised global palaeogeography from the breakup of Rodinia to the assembly of Gondwanaland, Sedimentary Geology, 294, 219-232.

Li, Z. Y., L. Ding, P. C. Lippert, and H. H. Wei (2013), Paleomagnetic constraints on the Cenozoic kinematic evolution of the Pamir plateau from the Western Kunlun Shan foreland, Tectonophysics, 603, 257-271.

Li, Y. X., L. S. Shu, B. Wen, Z. Y. Yang, and J. R. Ali (2013), Magnetic inclination shallowing problem and the issue of Eurasia's rigidity: insights following a palaeomagnetic study of upper Cretaceous basalts and redbeds from SE China, Geophysical Journal International, 194(3), 1374-1389.

Li, Y., Y. G. Song, L. B. Qian, X. M. Li, X. K. Qiang, and Z. S. An (2013), Paleomagnetic and Fission-Track Dating of a Late Cenozoic Red Earth Section in the Liupan Shan and Associated Tectonic Implications, Journal of Earth Science, 24(4), 506-518.

Li, Y. Q., D. Jia, A. Plesch, J. Hubbard, J. H. Shaw, and M. Wang (2013), 3-D geomechanical restoration and paleomagnetic analysis of fault-related folds: An example from the Yanjinggou anticline, southern Sichuan Basin, Journal of Structural Geology, 54, 199-214.

Li, H. B., D. Jia, L. Wu, Y. Zhang, H. W. Yin, G. Q. Wei, and B. L. Li (2013), Detrital zircon provenance of the Lower Yangtze foreland basin deposits: constraints on the evolution of the early Palaeozoic Wuyi-Yunkai orogenic belt in South China, Geological Magazine, 150(6), 959-974.

Lucifora, S., F. Cifelli, F. B. Rojay, and M. Mattei (2013), Paleomagnetic rotations in the Late Miocene sequence from the Cankiri Basin (Central Anatolia, Turkey): the role of strike-slip tectonics, Turkish Journal of Earth Sciences, 22(5), 778-792.

Martin, A. K. (2013), Double-saloon-door tectonics in the North Fiji Basin, Earth and Planetary Science Letters, 374, 191-203.

Muller, R. D., A. Dutkiewicz, M. Seton, and C. Gaina (2013), Seawater chemistry driven by supercontinent assembly, breakup, and dispersal, Geology, 41(8), 907-910.

Panaiotu, C. G., B. R. Jicha, B. S. Singer, A. Tugui, I. Seghedi, A. G. Panaiotu, and C. Necula (2013), Ar-40/Ar-39 chronology and paleomagnetism of Quaternary basaltic lavas from the Persani Mountains (East Carpathians), Physics of the Earth and Planetary Interiors, 221, 1-14.

Piper, J. D. A., F. Kocbulut, H. Gursoy, O. Tatar, L. Viereck, P. Lepetit, A. P. Roberts, and Z. Akpinar (2013), Palaeomagnetism of the Cappadocian Volcanic Succession, Central Turkey: Major ignimbrite emplacement during two short (Miocene) episodes and Neogene tectonics of the Anatolian collage, Journal of Volcanology and Geothermal Research, 262, 47-67.

Platt, J. P., and T. W. Becker (2013), Kinematics of rotating panels of E-W faults in the San Andreas system: what can we tell from geodesy?, Geophysical Journal International, 194(3), 1295-1301.

Powerman, V., A. Shatsillo, R. Coe, X. X. Zhao, D. Gladkochub, R. Buchwaldt, and V. Pavlov (2013), Palaeogeography of the Siberian platform during middle Palaeozoic Times (similar to 450-400 Ma): new palaeomagnetic evidence from the Lena and Nyuya rivers, Geophysical Journal International, 194(3), 1412-1440.

Rao, Y. H., M. Venkateshwarlu, G. Papanna, and B. R. Rao (2013), Palaeomagnetism of Khairmalia Volcanics, south of Chittorgarh - implications related to the basal age of the Proterozoic Vindhyan Supergroup, Current Science, 104(3), 364-367.

Rauch, M. (2013), The Oligocene-Miocene tectonic evolution of the northern Outer Carpathian fold-and-thrust belt: insights from compression-and-rotation analogue modelling experiments, Geological Magazine, 150(6), 1062-1084.

Ribeiro, P., P. F. Silva, P. Moita, Z. Kratinova, F. O. Marques, and B. Henry (2013), Palaeomagnetism in the Sines massif (SW Iberia) revisited: evidences for Late Cretaceous hydrothermal alteration and associated partial remagnetization, Geophysical Journal International, 195(1), 176-191.

Sen, K., and A. S. Collins (2013), Dextral transpression and late Eocene magmatism in the trans-Himalayan Ladakh Batholith (North India): implications for tectono-magmatic evolution of the Indo-Eurasian collisional arc, International Journal of Earth Sciences, 102(7), 1895-1909.

Shephard, G. E., R. D. Muller, and M. Seton (2013), The tectonic evolution of the Arctic since Pangea breakup: Integrating constraints from surface geology and geophysics with mantle structure, Earth-Science Reviews, 124, 148-183.

Torsvik, T. H., and L. R. M. Cocks (2013), Gondwana from top to base in space and time, Gondwana Research, 24(3-4), 999-1030.

Vernikovsky, V. A., N. L. Dobretsov, D. V. Metelkin, N. Y. Matushkin, and I. Y. Koulakov (2013), Concerning tectonics and the tectonic evolution of the Arctic, Russian Geology and Geophysics, 54(8), 838-858.

Vernikovsky, V. A., D. V. Metelkin, T. Y. Tolmacheva, N. A. Malyshev, O. V. Petrov, N. N. Sobolev, and N. Y. Matushkin (2013), Concerning the issue of paleotectonic reconstructions in the Arctic and of the tectonic unity of the New Siberian Islands Terrane: New paleomagnetic and paleontological data, Doklady Earth Sciences, 451(2), 791-797.

Prospecting and Surveying

Shah, A. K., P. A. Bedrosian, E. D. Anderson, K. D. Kelley, and J. Lang (2013), Integrated geophysical imaging of a concealed mineral deposit: A case study of the world-class Pebble porphyry deposit in southwestern Alaska, Geophysics, 78(5), B312-B323.

Van Dam, R. L., J. M. H. Hendrickx, N. J. Cassidy, R. E. North, M. Dogan, and B. Borchers (2013), Effects of magnetite on high-frequency ground-penetrating radar, Geophysics, 78(5), H1-H11.

Serpentinization

Chassefiere, E., B. Langlais, Y. Quesnel, and F. Leblanc (2013), The fate of early Mars' lost water: The role of serpentinization, Journal of Geophysical Research-Planets, 118(5), 1123-1134.

Frost, B. R., K. A. Evans, S. M. Swapp, J. S. Beard, and F. E. Mothersole (2013), The process of serpentinization in dunite from New Caledonia, Lithos, 178, 24-39.

Ogasawara, Y., A. Okamoto, N. Hirano, and N. Tsuchiya (2013), Coupled reactions and silica diffusion during serpentinization, Geochimica Et Cosmochimica Acta, 119, 212-230.

Prabhakar, N., and A. Bhattacharya (2013), Origin of zoned spinel by coupled dissolution-precipitation and inter-crystalline diffusion: evidence from serpentinized wehrlite, Bangriposi, Eastern India, Contributions to Mineralogy and Petrology, 166(4), 1047-1066.

Singh, N. I., L. D. Devi, and T. Y. Chanu (2013), Petrological and Geochemical Study of Serpentinised Peridotites from the Southern Part of Manipur Ophiolitic Complex, Northeast India, Journal of the Geological Society of India, 82(2), 121-132.

Synthesis

Ananth, K. P., S. P. Jose, K. S. Venkatesh, and R. Ilangovan (2013), Size Controlled Synthesis of Magnetite Nanoparticles Using Microwave Irradiation Method, Journal of Nano Research, 24, 184-193.

Emadi, H., and A. N. Kharat (2013), Single source preparation of superparamagnetic Fe3O4 nanoparticles by simple cyclic microwave approach, Materials Research Bulletin, 48(10), 3994-4001.

Gartman, A., and G. W. Luther (2013), Comparison of pyrite (FeS2) synthesis mechanisms to reproduce natural FeS2 nanoparticles found at hydrothermal vents, Geochimica Et Cosmochimica Acta, 120, 447-458.

Jiao, H., and J. L. Wang (2013), Single crystal ellipsoidal and spherical particles of alpha-Fe2O3: Hydrothermal synthesis, formation mechanism, and magnetic properties, Journal of Alloys and Compounds, 577, 402-408.

Spectroscopy and Microscopy

Caggiani, M. C., P. Colomban, C. Valotteau, A. Mangone, and P. Cambon (2013), Mobile Raman spectroscopy analysis of ancient enamelled glass masterpieces, Analytical Methods, 5(17), 4345-4354.

Fang, Y. K., W. Li, W. Sun, M. G. Zhu, Z. H. Guo, and B. S. Han (2013), Revealing of magnetic domains of strong bulk anisotropic permanent magnets via magnetic force microscopy, Journal of Magnetism and Magnetic Materials, 345, 176-179.

Koike, K. (2013), Spin-polarized scanning electron microscopy, Microscopy, 62(1), 177-191.

Lenaz, D., H. Skogby, A. M. Logvinova, N. V. Sobolev, and F. Princivalle (2013), A micro-Mossbauer study of chromites included in diamond and other mantle-related rocks, Physics and Chemistry of Minerals, 40(9), 671-679.

Marshall, C. P., and A. O. Marshall (2013), Raman Hyperspectral Imaging of Microfossils: Potential Pitfalls, Astrobiology, 13(10), 920-931.

Menard, M. C., K. J. Takeuchi, A. C. Marschilok, and E. S. Takeuchi (2013), Electrochemical discharge of nanocrystal-

line magnetite: structure analysis using X-ray diffraction and X-ray absorption spectroscopy, Physical Chemistry Chemical Physics, 15(42), 18539-18548.

Rodriguez-Fernandez, A., J. A. Blanco, S. W. Lovesey, V. Scagnoli, U. Staub, H. C. Walker, D. K. Shukla, and J. Strempfer (2013), Chiral properties of hematite alpha-Fe2O3 inferred from resonant Bragg diffraction using circularly polarized x rays, Physical Review B, 88(9).

Schaffert, S., B. Pfau, J. Geilhufe, C. M. Gunther, M. Schneider, C. V. Schmising, and S. Eisebitt (2013), High-resolution magnetic-domain imaging by Fourier transform holography at 21 nm wavelength, New Journal of Physics, 15.

A colleague of the GP community is Editor of Reviews of Geophysics

Fabio Florindo, research Director at the Istituto Nazionale di Geofisica e Vulcanologia (INGV) in Rome, and active member of the geomagnetic and paleomagnetic community, with research interests in Paleomagnetism and Environmental Magnetism with applications to paleoclimate, paleoceanography, geomagnetic field behaviour and tectonics, has been recently reappointed for a second term as editor for Reviews of Geophysics, from 2014 to 2017.

Reviews of Geophysics, at the top of the ISI cohort of Geochemistry and Geophysics for 14 years (IF 2013=13.906), provides an overview of geophysics and the directions in which it is going, and serves as an integrating force for the community. It distills and places in perspective previous scientific work in currently active subject areas of geophysics. Contributions that evaluate overall progress in the field and cover all disciplines embraced by AGU.

Reviews of Geophysics is an invitation only journal. If you would like to submit a manuscript for publication consideration, please write a cover letter describing how your manuscript would benefit the community of readers of the journal. For questions, contact reviews-geophysics@agu.org or Fabio Florindo directly.

The next Visiting Fellowship application deadline is April 30, 2014. Get on it!

University of Minnesota

The *IRM Quarterly* is always available as full color pdf online at www.irm.umn.edu

You can also follow us on facebook!

Review and Advisory Committee Announcement!

The IRM staff is pleased to announce that Dr. Brad Clement, (IODP and Texas A&M) and Dr. Aleksey Smirnov (Michigan Tech) have accepted to join the IRM's Review and Advisory Committee (RAC).

After over four years of outstanding service we thank Dr. Catherine Constable, the outgoing committee Chair, and Dr. Andrew Roberts. We also congratulate (and thank) Dr. Suzanne McEnroe for having accepted to serve as the new committee Chair!

The new appointments were suggested at the last RAC meeting held at the IRM on September 27th.

The new committee will be composed of:

Dr. Suzanne McEnroe, Chair- Norwegian University of Science and Technology
Dr. Stefanie Brachfeld- Montclair State University
Dr. Brad Clement- IODP and Texas A&M
Dr. Chris Leighton- University of Minnesota
Dr. Yongxin Pan- Institute of Geology & Geophysics, Chinese Academy of Sciences
Dr. Aleksey Smirnov- Michigan Tech
Dr. Benjamin Weiss- Massachusetts Institute of Technology.

The role of the RAC is to provide external review and insight into ways the IRM can better serve the rock magnetic community, and to evaluate Visiting Fellows applications. Members come from all over the world and serve 2-6 year terms, meeting twice a year: once at a major meeting, such as AGU, and once here in beautiful Minneapolis.

IRM

... cont'd. from pg. 1.

carrying remanence at or above room temperature; determines how much M is recovered after a full cooling and heating cycle; allows determining domain state; allows estimating amount of oxidation from shape of heating curve (Özdemir and Dunlop, 2010)

A variation of this sequence proposed by David Dunlop is to cycle the low temperature demagnetization through incremental steps. Doing so enables evaluation of the reversibility of the cooling and heating curves for minerals with different unblocking temperatures/transitions, thus enabling a better understanding of the specimen.

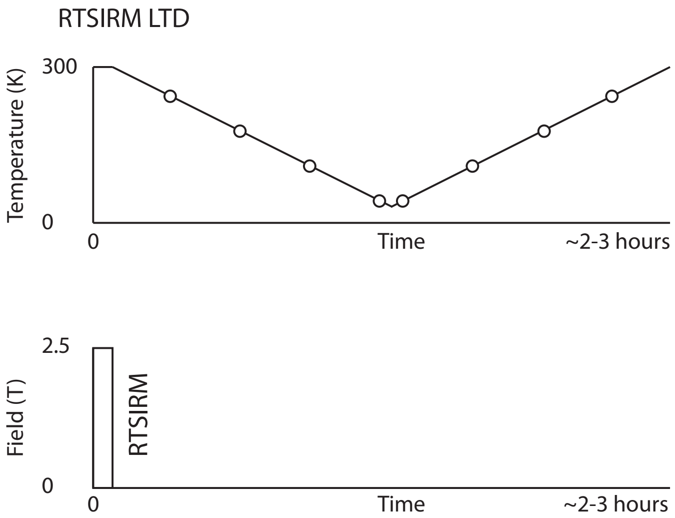

Figure 1. Schematic of Room Temperature SIRM Low-Temperature Demagnetization sequence (open circles represent measurements steps, typically every 5-10 K).

NRM LTD

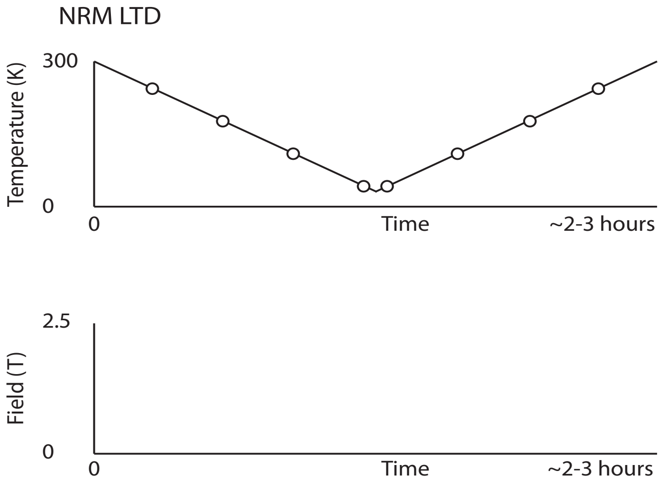

Figure 3. Low-Temperature Demagnetization of the initial state of the specimen (here generically termed NRM, but this may be an NRM, an ARM, an IRM, a TRM, etc.) (open circles represent measurements steps, typically every 5-10 K).

An other variant of the previous sequence is to measure the pre-existing remanence of the specimen (no field is applied by the MPMS) during low-temperature demagnetization and the subsequent recovery of the magnetization upon warming back to room temperature. The initial state of the specimen is thus measured, whether this is an NRM, ARM, IRM, TRM, etc. (Muxworthy *et al*., 2003) (figure 3). Reminding the reader that the MPMSs only detect the axial moment, this will not be the total magnetization unless the specimen is cut and measured along its characteristic remanent magnetization (ChRM) direction (e.g. Liu *et al*., 2003).

Advantages: characterizes phases capable of carrying remanence at or above room temperature; allows observation of low-temperature transitions on different remanent states, and their dependence on other experimental values (grainsize, composition, …).

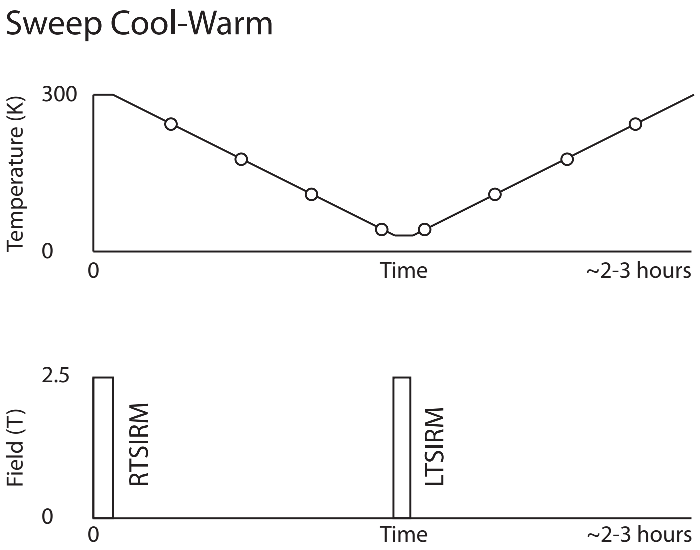

Figure 4. Schematic of Sweep-Cool-Warm sequence (open circles represent measurements steps, typically every 5-10 K). Such experiment generates the ZFC remanence and RT remanence on cooling curves in figure 2. Curves possess different shapes and spacing depending on magnetic mineralogy, oxidation and domain state (see text below for details).

Sweep-Cool-Warm

A very effective and "rapid" first-measurement to perform on a specimen, it involves imparting a room T SIRM (typically 2.5 T) and measuring the (loss of) remanence during cooling to a preset temperature, typically 20 K (upper and lower graphs on figure 4, left hand side). While at cold temperature, a second, same field SIRM is imparted (right hand side of graphs in figure 4) and the remanence is measured on heating back to room T. Note that this second curve is the same as that generated by other sequences and termed "zero-field cooled (ZFC) LTSIRM". The duration of this experiment is also ~2.5 hours.

Advantages: rapid; provides information on phases with blocking temperatures or ordering temperatures below 300 K; approaches transitions from both directions; both SIRM enhance transitions on both curves; allows estimating amount of oxidation from shape of heating curve (Özdemir and Dunlop, 2010) (see Mineral Diagnostics paragraph below).

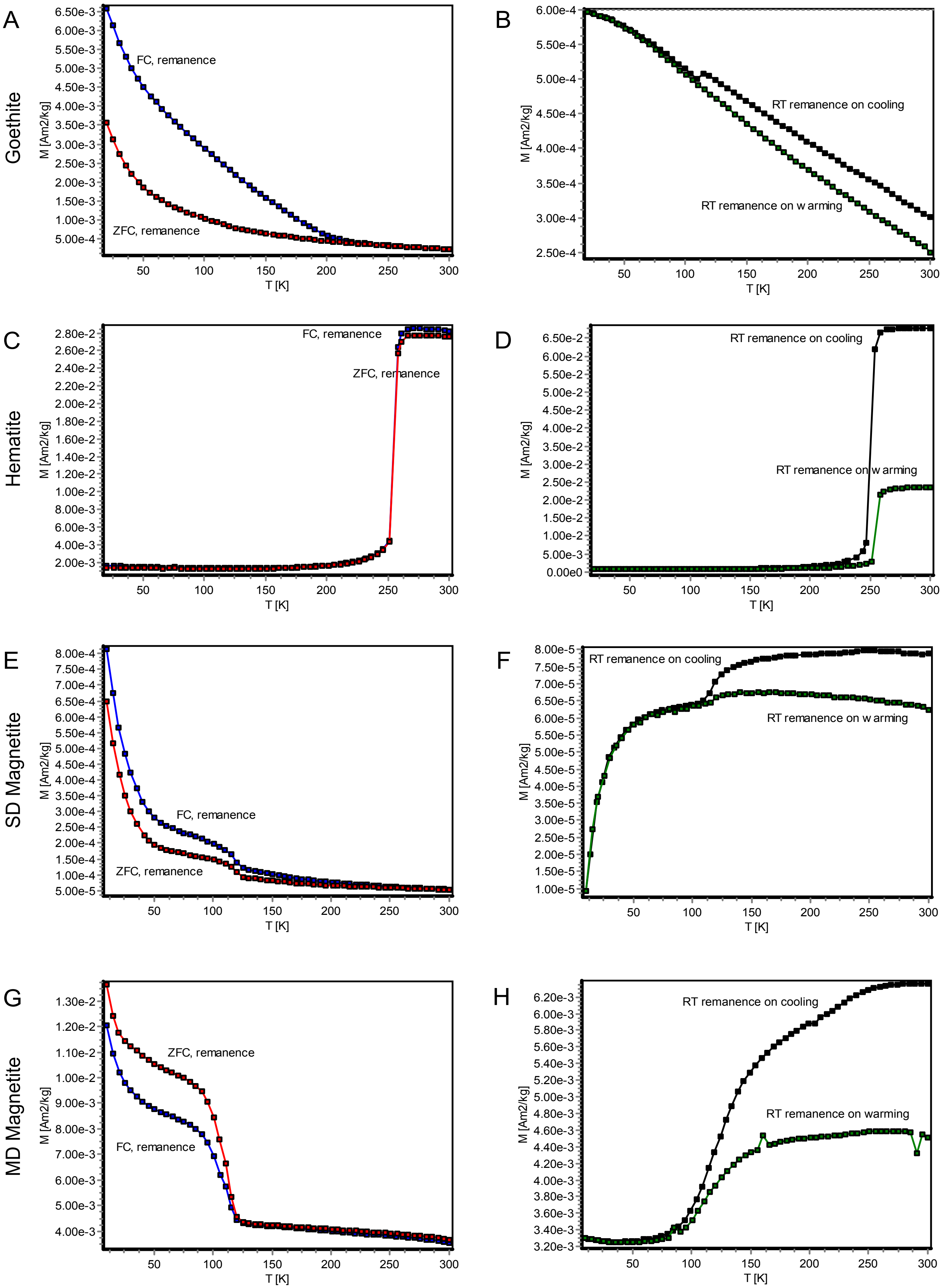

Figure 2. Typical low-temperature remanent curves for common magnetic minerals: Goethite, Hematite, Single Domain (SD) Magnetite and Multi Domain (MD) Magnetite. On the left-hand column are the Field-cooled and Zero Field-cooled remanence curves, whereas on the right-hand side are the Room temperature remanence curves on cooling and warming (see text for details).

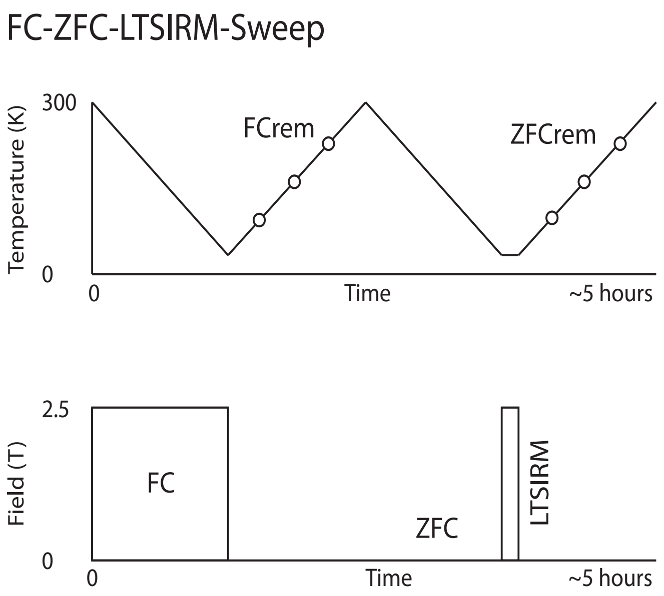

Figure 5. Field-Cooled, Zero Field-Cooled Low-Temperature SIRM Sweep sequence (open circles represent measurements steps, typically every 5-10 K). This experiment generates the FC remanence and ZFC remanence curves shown in figure 2, which possess different shapes and spacing depending on magnetic mineralogy, oxidation and domain state (see text below for details). Some sequences by the same name also measure in-field magnetization on cooling at the beginning of the sequence run (not shown in either figure).

FC-ZFC-LTSIRM-sweep

A sustained DC field (typically 2.5 T) is imparted on the specimen while this cools from room to low temperature (field-cooled). Certain sequences measure the in-field magnetization on cooling, which often is dominated by the paramagnetic response (when paramagnets are present). The field is switched off at cold temperature and the magnetic remanence is measured as the specimen warms back up to room temperature (FC remanence, left hand side of figure 5). The specimen is subsequently cooled in a null magnetic field (ZFC), an LTSIRM is imparted and the remanence is measured again on warming back up to room T (ZFC remanence, middle section of figure 5). This second curve, as mentioned earlier is the LTSIRM remanence measured on warming in the second part of the "Sweep-Cool-Warm" sequence. Such an experiment lasts approximately 5 hours.

Advantages: detect goethite; distinguish between SD and MD magnetite; evaluate state of oxidation (Özdemir and Dunlop, 2010) (see Mineral Diagnostics paragraph below).

FC-ZFC-LTSIRM-RTSIRM LTD

A variation on the previous sequence is the addition of the RTSIRM LTD sequence at the end, resulting in a longer (8-9 hours), more detailed sequence to be run on specimens for which more information needs to be extracted. After the first FC-ZFC-LTSIRM part of the experiment (previous sequence), the RTSIRM (first experiment described) sequence is performed (figure 6).

Advantages: detects goethite; approaches transitions from both sides; distinguishes between SD and MD magnetite; evaluates state of oxidation (Özdemir and Dunlop, 2010) (see Mineral Diagnostics paragraph below).

FC LTSIRM and RTSIRM LTD

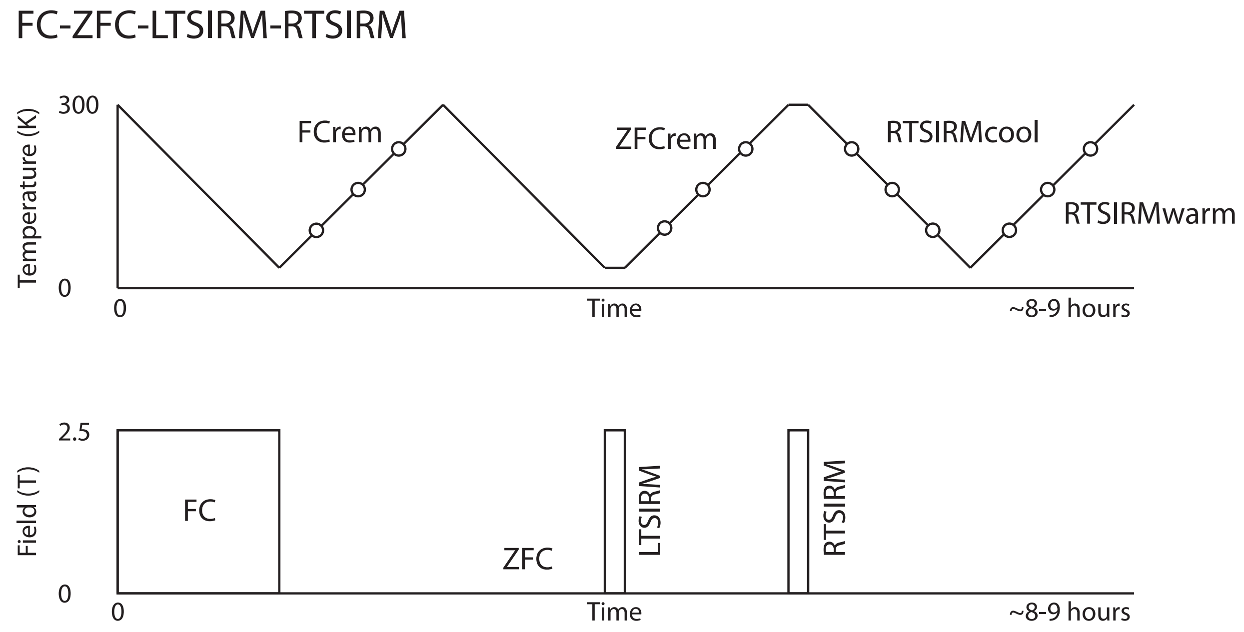

Figure 6. Schematic of Field-Cooled, Zero Field-Cooled Low-Temperature SIRM and Room Temperature SIRM sequence (open circles represent measurements steps, typically every 5-10 K). This experiment generates the FC remanence, ZFC remanence, RT remanence on cooling and RT remanence on heating curves shown in figure 2, which possess different shapes and spacing depending on magnetic mineralogy, oxidation and domain state (see text below for details).

A slightly shorter sequence than the previous, eliminates the ZFC–remanence measurement (figure 7). It is therefore not possible to identify goethite from the FC/ZFC ratio and the domain state is only evaluated from the RTSIRM curves, together with oxidation state.

Other sequences

Other types of experiments are often performed, but will not be described too zealously here, because they are more readily intuitive or because not all are too commonly performed by rock-magnetists, but are instead of more interest to engineers or material scientists.

FC-ZFC (induced M on heating)

This sequence measures the in-field magnetization after both field and zero field-cooling (the field strength applied for the measurements is typically a few mT). It is particularly useful to determine blocking transitions in superparamagnetic nano particles and is therefore typically mostly used by material scientist and engineers. The duration of such experiment is approximately 5 hours.

AC(f,H,T)

A completely different set of experiments are measurements of AC susceptibility at different frequencies and in different field intensities as a function of temperature. Both in-phase and out-of-phase susceptibilities are measured (see Jackson, Jackson *et al.* and Bowles *et al.* in IRM Quarterlies 13-4, 14-3, 19-3). These experiments typically require between 12 hours (5 different frequencies and 1 fixed field amplitude) and 48 hours (5 frequencies and 4 amplitudes).

Loops

Hysteresis loops may be measured on the MPMPS at different temperatures and up to different field intensities. A drawback of measuring hysteresis loops on the MPMS is the time involved, which makes vibrating sample magnetometers (VSMs) a more efficient instrument for measuring loops, thought these are not always set to operate at temperatures other than room T. MPMS loops make sense when fields > 2 T or temperatures < 10 K are required.

Goethite test

Sequences designed to isolate the magnetic contribution of goethite exist. These are performed on MPSMs that go up to 400 K (like *Big Red*), allowing thermal demagnetization of goethite (Néel temperature, T_N= ~390 K (~120 °C). Different sequences exist, which are essentially variations of this routine: fully magnetizing a specimen in high fields (5 T) in the MPMS (but could be done in a pulse magnetizer or other instrument capable of reaching such high fields). The specimen is then removed from the MPMS and is AF demagnetized in fields of ~200 mT to fully eliminate the contribution of magnetite. Back in the MPMS, the remanence is measured upon cooling from 300 K to low temperatures (~20 K) and then remeasured upon heating past goethite's Néel temperature to 400 K, to fully demagnetize the goethite. The specimen is subsequently measured again upon cooling back to low temperatures, which should show no remaining remanence in the absence of other phases (Carter-Stiglitz *et al*., 2006a; Guyodo *et al.*, 2006; Lascu and Feinberg, 2011).

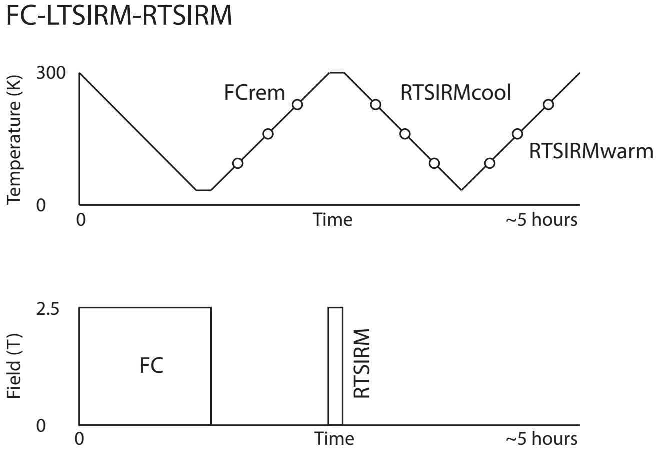

Figure 7. Field-Cooled, and Room Temperature SIRM sequence scheme (open circles represent measurements steps, typically every 5-10 K). This experiment generates the FC remanence, RT remanence on cooling and RT remanence on heating curves shown in figure 2, which possess different shapes and spacing depending on magnetic mineralogy, oxidation and domain state (see text below for details). Some sequences by the same name may also measure in-field magnetization on cooling at the beginning of the sequence run (not shown in either figure).

Mineral Diagnostics

Figure 2 shows characteristic remanence curves for different common magnetic minerals. On the left-hand side are the FC and ZFC remanences, whereas on the right are the RT remanences on cooling and warming.

Goethite's diagnostic features are a wide spread between the FC and ZFC remanences, with FC being usually at least twice the ZFC. Although the T_C of goethite is ~390 K, it is not uncommon to observe goethite demagnetize at lower temperatures, even 200 K as in figure 2a. RTSIRM curves for goethite increase in intensity going towards lower temperatures and are reversible. The heating curve remaining below the cooling curve in figure 2b, with loss of remanence below ~120 K is indication of some magnetite in this specimen (see description for magnetite below).

The most diagnostic feature for hematite is the Morin transition, around 250-260 K (see Bowles *et al.* in IRM Quarterly 20-1). Below these temperatures the canted anti-ferromagnetism becomes a perfect antiferromagnetism and only a weak defect moment remains, therefore the remanence is strongly decreased. The Morin transition is apparent in all curves in figures 2c, d, however note the scale on the M axes: FC and ZFC remanences have approximately the same magnitude which is in between the RT remanences on cooling (higher) and heating (lower). Reduced grainsize and titanium substitutions have the effect of lowering the temperature or suppressing the occurrence of the Morin transition.

Low temperature remanence curves for magnetite possess a very diagnostic feature around 120 K. This is the Verwey transition (T_V) (see Jackson *et al.* a, b and Bowles *et al.* in the IRM Quarterlies 20-4, 21-4, 22-2) which corresponds to a transformation from a cubic crystal structure at $T > T_V$ to monoclinic $< T_V$. The Verwey transition is apparent from both the FC/ZFC and RT remanence curves, however, the isotropic point (T_i= ~130 K), which accompanies a change in sign of the magnetocrystalline anisotropy constant (K1) is approached faster upon cooling and therefore it often appears sharper on the RT remanence on cooling and warming curves. As for hematite, even small amounts of titanium eliminate the transition, but isotropic points still remain (Moskowitz *et al*., 1998; Carter-Stiglitz *et al*., 2006).

For SD magnetite grains the FC remanence curve is always higher than the ZFC remanence (figure 2e), whereas the opposite is true for MD grains (figure 2g). SD grains also show more recovery of magnetization when performing a thermal demagnetization of a RTSIRM (figure 2f), while MD grains exhibit a substantially lower remanence on heating curve (figure 2h).

The shapes of the RT remanence curves are also indicative of maghemitization (oxidation). Increased humpiness of these curves is indicative of maghemite (Özdemir and Dunlop, 2010).

Other minerals that are not shown in figure 2 also possess diagnostic features.

Pyrrhotite ($Fe_{(1-x)}S$, x= 0- 0.2) possesses a transition at 35 K (see Rochette *et al.* in IRM Quarterly 21-1). As for magnetite, MD grains lose more of their remanence on cooling than SD grains, resulting in a greater spread of the RT remanence curves.

Ilmenite ($FeTiO_3$) possesses a 70 K ordering temperature (see Fabian et al. in IRM Quarterly 17.4)

Troilite (FeS) has a transition at 60-75 K (Kohout *et al.*, 2007)

Daubreelite ($FeCr_2S_4$) has an ordering temperature of 150-170 K (Kohout et al., 2007)

Chromite ($FeCr_2O_4$) 75 K (see Baezeva in IRM Quarterly 22-4; Gattacceca *et al.*, 2011).

Caveats

While many transitons are diagnostic of mineralogical transformations, one must exercise caution when interpreting low-temperature data because features that may appear to be transitions are often not diagnostic of anything that we know of. For example, it is not uncommon to observe a decrease in remanence around 50 K in both FC and ZFC remanence curves which does not correspond to any known mineralogical transition; in some cases it is due to paramagnetic moments in the imperfect zero field of the MPMS.

References

Carter-Stiglitz, B., Banerjee, S.K., Gourlan, A., Oches, E., 2006a. A multi-proxy study of Argentina loess: Marine oxygen isotope stage 4 and 5 environmental record from pedogenic hematite. Palaeogeogr. Palaeoclimatol. Palaeoecol., 239, 45-62.

Carter-Stiglitz, B., Moskowitz, B., Solheid, P., Berquo, T.S., Jackson, M., Kosterov, A., 2006b. Low-temperature magnetic behavior of multidomain titanomagnetites: TM0, TM16, and TM35, J. Geophys. Res., 111, B12S05, doi:10.1029/2006JB004561.

Dunlop, D.J. and Özdemir, Ö., 1997. Rock Magnetism: Fundamentals and frontiers. Cambridge Studies in Magnetism, Cambridge University Press, Cambridge, 573 pp.

Gattacceca, J., Rochette, P., Lagroix, F., Mathe', P.-E., Zanda, B., 2011. Low temperature magnetic transition of chromite in ordinary chondrites, Geophys, Res. Lett., 38, L10203.

Guyodo, Y., LaPara, T.M., Anschutz, A.J., Penn, R.L., Banerjee, S.K., Geiss, C.E., Zanner, W., 2006. Rock magnetic, chemical and bacterial community analysis of a modern soil from Nebraska, Earth Planet. Sci. Lett., 251, 168-178.

IRM Quarterlies: 13-4; 14-3; 17-4 ; 19-3; 20-1; 20-4; 21-4; 22-2; 22-4.

Kohout, T., Kosterov, A., Jackson, M., Pesonen, L. J., Kletetschka, G. & Lehtinen, M. 2007, Low-temperature magnetic properties of the Neuschwanstein EL6 meteorite, Earth and Planet. Sci. Lett., 261, 1-2, 143-151.

Liu, Q., Jackson, M., Banerjee, S.K., Zhu, R., Pan, Y., Chen, F., 2003. Determination of magnetic carriers of the characteristic remanent magnetization of Chinese loess by low-temperature demagnetization, Earth Planet. Sci. Lett., 216, 175-186.

Moskowitz, B.M., Jackson, M., Kissel, C., 1998. Low-temperature magnetic behavior of titanomagnetites. Earth Planet. Sci. Lett., 157, 141-149.

Muxworthy, A., Dunlop, D.J., Özdemir, Ö., 2003. Low-temperature cycling of isothermal and anhysteretic remanence: microcoercivity and magnetic memory, Earth Planet. Sci. Lett., 205, 173-184.

Özdemir, Ö., and Dunlop, D. J., 2010. Hallmarks of maghemitization in low-temperature remanence cycling of partially oxidized magnetite nanoparticles, J. geophys. Res., 115, B02101, doi:10.1029/2009JB006756

The MPMS lab: *Old Blue* in the foreground, *Big Red* in the middle and the helium liquefier in the background.

University of Minnesota
291 Shepherd Laboratories
100 Union Street S. E.
Minneapolis, MN 55455-0128
phone: (612) 624-5274
fax: (612) 625-7502
e-mail: irm@umn.edu
www.irm.umn.edu

The IRM Quarterly

The *Institute for Rock Magnetism* is dedicated to providing state-of-the-art facilities and technical expertise free of charge to any interested researcher who applies and is accepted as a Visiting Fellow. Short proposals are accepted semi-annually in spring and fall for work to be done in a 10-day period during the following half year. Shorter, less formal visits are arranged on an individual basis through the Facilities Manager.

The *IRM* staff consists of **Subir Banerjee**, Professor/Founding Director; **Bruce Moskowitz**, Professor/Director; **Joshua Feinberg**, Assistant Professor/Associate Director; **Mike Jackson, Peat Sølheid** and **Dario Bilardello**, Staff Scientists.

Funding for the *IRM* is provided by the **National Science Foundation**, the **W. M. Keck Foundation**, and the **University of Minnesota**.

The *IRM Quarterly* is published four times a year by the staff of the *IRM*. If you or someone you know would like to be on our mailing list, if you have something you would like to contribute (*e.g.*, titles plus abstracts of papers in press), or if you have any suggestions to improve the newsletter, please notify the editor:

Dario Bilardello
Institute for Rock Magnetism
University of Minnesota
291 Shepherd Laboratories
100 Union Street S. E.
Minneapolis, MN 55455-0128
phone: (612) 624-5274
fax: (612) 625-7502
e-mail: dario@umn.edu
www.irm.umn.edu